

B -hadron fragmentation functions at next-to-next-to-leading order from global analysis of e^+e^- annihilation data

Maral Salajegheh,^{1,*} S. Mohammad Moosavi Nejad,^{1,2,†} Hamzeh Khanpour,^{3,2,‡} Bernd A. Kniehl,^{4,§} and Maryam Soleymaninia^{5,2,¶}

¹*Faculty of Physics, Yazd University, P. O. Box 89195-741, Yazd, Iran*

²*School of Particles and Accelerators, Institute for Research in Fundamental Sciences (IPM), P. O. Box 19395-5531, Tehran, Iran*

³*Department of Physics, University of Science and Technology of Mazandaran, P. O. Box 48518-78195, Behshahr, Iran*

⁴*II. Institut für Theoretische Physik, Universität Hamburg, Luruper Chaussee 149, 22761 Hamburg, Germany*

⁵*Department of Physics, Shahid Rajaei Teacher Training University, Lavizan, Tehran 16788, Iran*

(Dated: May 13, 2019)

We present nonperturbative fragmentation functions (FFs) for bottom-flavored (B) hadrons both at next-to-leading (NLO) and, for the first time, at next-to-next-to-leading order (NNLO) in the $\overline{\text{MS}}$ factorization scheme with five massless quark flavors. They are determined by fitting all available experimental data of inclusive single B -hadron production in e^+e^- annihilation, from the ALEPH, DELPHI, and OPAL Collaborations at CERN LEP1 and the SLD Collaboration at SLAC SLC. The uncertainties in these FFs as well as in the corresponding observables are estimated using the Hessian approach. We perform comparisons with available NLO sets of B -hadron FFs. We apply our new FFs to generate theoretical predictions for the energy distribution of B hadrons produced through the decay of unpolarized or polarized top quarks, to be measured at the CERN LHC.

PACS numbers: 13.66.Bc,13.85.Ni,13.87.Fh,14.40.Nd

* M.Salajegheh@stu.yazd.ac.ir

† Mmoosavi@yazd.ac.ir

‡ Hamzeh.Khanpour@mail.ipm.ir

§ kniehl@desy.de

¶ Maryam_Soleymaninia@ipm.ir

CONTENTS

I. Introduction	2
II. QCD framework for B -hadron FFs	4
III. Determination of B -hadron FFs and their uncertainties	6
IV. Results and discussion	8
V. B -hadron production by top-quark decay	11
VI. Summary and Conclusions	15
Acknowledgments	17
References	17

I. INTRODUCTION

For a long time, there has been considerable interest in the study of bottom-flavored-hadron (B -hadron) production at hadron and e^+e^- colliders, both experimentally and theoretically. Historically, the first measurements were performed more than three decades ago by the UA1 Collaboration at the CERN $S\bar{p}\bar{p}S$ collider [1] operating at center-of-mass (CM) energy $\sqrt{s} = 630$ GeV.

In the framework of the parton model of QCD, the description of the inclusive single production of identified hadrons h involves fragmentation functions (FFs), $D_a^h(x, Q^2)$. At leading order, their values correspond to the probability that the colored parton a , which is produced at short distance, of order $1/\sqrt{Q^2}$, fragments into the colorless hadron h carrying the fraction x of the energy of a . Given their x dependence at some scale Q_0 , the evolution of the FFs with Q^2 may be computed perturbatively from the timelike

Dokshitzer-Gribov-Lipatov-Altarelli-Parisi (DGLAP) equations [2–4]. The timelike splitting functions $P_{a \rightarrow b}^T(x, \alpha_s(Q^2))$ appearing therein are known through NNLO [5–7]. In the case of e^+e^- annihilation, the hard-scattering cross sections for the inclusive production of parton a , to be convoluted with $D_a^h(x, Q^2)$, are also known through NNLO [5, 8–11]. This allows one to interpret e^+e^- data of the inclusive single production of hadron h at NNLO and thus to extract FFs at this order [12–15]. Owing to the factorization theorem, the FFs are independent of the process by which parton a is produced. This allows one to transfer experimental information from e^+e^- annihilation to any other production mechanism, such as photoproduction, leptonproduction, hadroproduction, and two-photon scattering. Of all these processes, e^+e^- annihilation provides the cleanest laboratory for the extraction of FFs, being devoid of nonperturbative effects beyond fragmentation itself. Presently, there is particular interest in hadroproduction at the BNL Relativistic Heavy Ion Collider (RHIC) and the CERN Large Hadron Collider (LHC) due to ongoing experiments.

The parton model of QCD implemented in the modified minimal-subtraction ($\overline{\text{MS}}$) factorization scheme with n_f massless-quark flavors, the so-called zero-mass variable-flavor-number scheme (ZM-VFNS), can also be applied to the open production of heavy flavors, such as D and B hadrons, provided the hard energy scale characteristic for the production process is sufficiently larger than the heavy-flavor mass. This is certainly the case for all the applications here, because $M_B \ll M_Z, m_t$. Recently, D hadron FFs have been provided at NNLO in Ref. [16]. Here, we perform the first NNLO determination of B -hadron FFs.

In Refs. [17, 18], B -hadron FFs were extracted at NLO in the ZM-VFNS by fitting to the fractional-energy distributions $d\sigma/dx_B$ of the cross section of $e^+e^- \rightarrow B + X$ measured by the ALEPH [19] and OPAL [20] Collaborations at the CERN Large Electron Positron Collider (LEP1) and the SLD Collaboration [21] at the SLAC Linear Collider (SLC).

In the meantime, also the DELPHI Collaboration have reported a similar measurement at LEP1 [22]. In the present work, these data are, for the first time, included in a B -hadron

FF fit. On the other hand, we are not aware of any other such data from e^+e^- annihilation. In want of NNLO hard-scattering cross sections for inclusive single B -hadron production from other initial states, we do concentrate here on e^+e^- annihilation. We also go beyond Refs. [17, 18] by performing a full-fledged error estimation, both for the FFs and the resulting differential cross sections, using the Hessian approach [23].

The LEP1 experiments [19, 20, 22] identified the B hadrons by their semileptonic decays, $B \rightarrow D^{(*)}\ell\nu$, while the SLD Collaboration [21] collected an inclusive sample of reconstructed B -hadron decay vertices. The bulk of the experimentally observed B hadrons is made up by B^\pm , B^0/\bar{B}^0 , and B_s^0/\bar{B}_s^0 mesons.

The outline of this paper is as follows: In Section II, we describe the theoretical framework of inclusive single hadron production in e^+e^- annihilation through NNLO in the ZM-FVNS and introduce our parametrization of the $b/\bar{b} \rightarrow B$ FF at the initial scale. In Section III, we explain the minimization method in our analysis and our approach to error estimation. In Section IV, our NLO and NNLO results are presented and compared with the experimental data fitted to. In Section V, we present our NLO predictions for the normalized-energy distributions of B hadrons from decays of (un)polarized top quarks. Our conclusions are given in Section VI.

II. QCD FRAMEWORK FOR B -HADRON FFS

As mentioned in Sec. I, we fit nonperturbative B -hadron FFs to measured x_B distributions of the cross section of

$$e^+e^- \rightarrow (\gamma^*, Z) \rightarrow B + X, \quad (1)$$

where X refers to the unobserved part of the final state. In the following, we explain how to evaluate the cross section of process (1) at NLO and NNLO in the ZM-VFNS. Denoting the four-momenta of the virtual gauge boson and the B hadron by q and p_B , respectively, we have $s = q^2$, $p_B^2 = m_B^2$, and $x_B = 2(p_B \cdot q)/q^2$. In the CM frame, $x_B = 2E_B/\sqrt{s}$ is the energy

of the B hadron in units of the beam energy. In the ZM-VFNS, we have

$$\frac{1}{\sigma_{\text{tot}}} \frac{d\sigma}{dx_B}(e^+e^- \rightarrow B + X) = \sum_i \int_{x_B}^1 \frac{dx_i}{x_i} \frac{1}{\sigma_{\text{tot}}} \frac{d\sigma_i}{dx_i}(x_i, \mu_R, \mu_F) D_i^B\left(\frac{x_B}{x_i}, \mu_F\right), \quad (2)$$

where $i = g, u, \bar{u}, \dots, b, \bar{b}$ runs over the active partons with four-momenta p_i , $d\sigma_i(x_i, \mu_R, \mu_F)/dx_i$ is the partonic cross section of $e^+e^- \rightarrow i + X$ differential in $x_i = 2(p_i \cdot q)/q^2$, $D_i^B(z, \mu_F)$ is the $i \rightarrow B$ FF, and μ_R and μ_F are the renormalization and factorization scales, respectively. The latter are a priori arbitrary, but a typical choice is $\mu_F = \mu_R = \sqrt{s}$. In the CM frame, $z = x_B/x_i$ is the fraction of energy passed on from parton i to the B hadron. It is customary in experimental analyses to normalize Eq. (2) by the total hadronic cross section,

$$\sigma_{\text{tot}} = \frac{4\pi\alpha^2(s)}{s} \left(\sum_i^{n_f} \tilde{e}_i^2(s) \right) \left(1 + \alpha_s K_{\text{QCD}}^{(1)} + \alpha_s^2 K_{\text{QCD}}^{(2)} + \dots \right), \quad (3)$$

where α and α_s are the fine-structure and strong-coupling constants, respectively, \tilde{e}_i is the effective electroweak charge of quark i , and the coefficient $K_{\text{QCD}}^{(n)}$ contains the N^n LO correction. Here, we need $K_{\text{QCD}}^{(1)} = 3C_F/(4\pi)$ and $K_{\text{QCD}}^{(2)} \approx 1.411$ [24].

The z distribution of the $b \rightarrow B$ FF at the starting scale μ_0 is a genuinely nonperturbative quantity to be extracted from experimental data. Its form is unknown, and an educated guess is in order. The selection criterion is to score a minimum χ^2 value as small as possible with a set of fit parameters as minimal as possible. As in Refs. [17, 18], we adopt here the simple power ansatz [25],

$$D_b^B(z, \mu_0) = N_b z^{\alpha_b} (1-z)^{\beta_b}, \quad (4)$$

with fit parameters N_b , α_b , and β_b , and choose $\mu_0 = m_b = 4.5$ GeV. This ansatz was found to enable excellent fits [17, 18]. The $i \rightarrow B$ FFs for the other quarks and the gluon are assumed to be zero at $\mu_F = \mu_0$ and are generated through the DGLAP evolution to larger values of μ_F . We take $\alpha_s(M_Z)$ to be an input parameter and adopt the world average value 0.1181 for $n_f = 5$ [26] both at NLO and NNLO.

As mentioned in Sec. I, we fit to ALEPH [19], DELPHI [22], OPAL [20], and SLD [21] data. These data sets reach down to very small x_B values, which fall outside the range of

validity of our fixed-order approach. In fact, in the small- x_B limit, both the timelike splitting functions and the hard-scattering cross sections develop soft-gluon logarithms that require resummation. At the same time, finite- m_b and finite- M_B effects become relevant there. We leave the implementation of these refinements for future work, and instead impose appropriate minimum- x_B cuts for the time being. Specifically, we only include ALEPH data points with $x_B \geq 0.25$, DELPHI data points with $x_B \geq 0.36$, OPAL data points with $x_B \geq 0.325$, and SLD data points with $x_B \geq 0.28$. This enables acceptable fits within the fit range, at the expense of certain deviations in the small- x_B range, of course. The fixed-order approach is also challenged in the large- x_B limit, by the emergence of threshold logarithms, which also require resummation. In practice, however, these effects do not jeopardize the quality of our fits, so that we refrain from imposing maximum- x_B cuts.

III. DETERMINATION OF B -HADRON FFS AND THEIR UNCERTAINTIES

We now explain our fitting procedure. For a given set $p = \{N_b, \alpha_b, \beta_b\}$ of fit parameters, the goodness of the overall description of the experimental data by the theoretical predictions is measured by the global χ^2 value,

$$\chi_{\text{global}}^2(p) = \sum_{n=1}^{N^{\text{exp}}} w_n \chi_n^2(p), \quad (5)$$

where n labels the $N^{\text{exp}} = 4$ experimental data sets, w_n are their weight factors [27, 28], which we take to be unity, and

$$\chi_n^2(p) = \left(\frac{1 - \mathcal{N}_n}{\Delta \mathcal{N}_n} \right)^2 + \sum_{i=1}^{N_n^{\text{data}}} \left(\frac{\mathcal{N}_n \mathcal{F}_{n,i}^{\text{exp}} - \mathcal{F}_{n,i}^{\text{theo}}(p)}{\mathcal{N}_n \Delta \mathcal{F}_{n,i}^{\text{exp}}} \right)^2 \quad (6)$$

is the χ^2 value of data set n . On the experimental side, $\mathcal{F}_{n,i}^{\text{exp}}$ is the central value of $(1/\sigma_{\text{tot}})d\sigma/dx_B$ measured in bin i out of the N_n^{data} bins in data set n , $\Delta \mathcal{F}_{n,i}^{\text{exp}}$ is its individual error obtained by combining statistical and systematic errors in quadrature, \mathcal{N}_n is the unknown overall normalization factor of data set n to be fitted, and $\Delta \mathcal{N}_n$ is its error as

quoted by the experimental collaboration. On the theoretical side, $\mathcal{F}_{n,i}^{\text{theo}}(p)$ is the respective NLO or NNLO prediction.

We determine the fit parameters p by minimizing Eq. (5) with the help of the Monte Carlo package MINUIT [29] from the CERN program library. We adopt a two-step procedure. In the pre-fitting stage, we determine the four values \mathcal{N}_n by fitting them simultaneously with the three fit parameters p . In the main fitting stage, we then refine the determination of p with large statistics keeping \mathcal{N}_n fixed. In the evaluation of $\chi_{\text{global}}^2(p)/\text{d.o.f.}$, we take the number of degrees of freedom to be the overall number of data points fitted to minus three for the proper fit parameters p . We find the APFEL library [30] to be a very useful FF fitting tool.

We now describe our methodology for the estimation of the uncertainties in the B -hadron FFs. We adopt the Hessian approach to the propagation of uncertainties from the experimental data sets to the FFs, which has proven of value in global analyses of parton distribution functions and has been frequently applied there. For definiteness, we ignore additional sources of uncertainties, which are mostly of theoretical origin and are negligible against the experimental uncertainties taken into account here. In the following, we briefly review our procedure. For more details, we refer to Ref. [31].

In the Hessian approach, the uncertainty bands on the B -hadron FFs, $\Delta D_b^B(z)$, may be obtained through linear error propagation,

$$[\Delta D^B(z)]^2 = \Delta\chi_{\text{global}}^2(\hat{p}) \sum_{i,j} \frac{\partial \Delta D^B(z, \hat{p})}{\partial p_i} H_{ij}^{-1}(\hat{p}) \frac{\partial \Delta D^B(z, \hat{p})}{\partial p_j}, \quad (7)$$

where p_i ($i = 1, 2, 3$) are the free parameters in Eq. (4), \hat{p}_i are their optimized values, and $H^{-1}(p)$ is the covariance matrix, which is a default output of the MINUIT program [29]. In Eq. (7), we have suppressed the label μ_F for the factorization scale, which we take to be μ_0 . The error bands $\Delta D^B(z)$ are subject to DGLAP evolution in μ_F along with the central values $D^B(z)$. The confidence level (C.L.) is controlled by $T^2 = \Delta\chi_{\text{global}}^2$. We adopt the standard parameter fitting criterion by choosing $T = 1$, which corresponds to the 68% C.L., i.e. the

1σ error band. In Sec. IV, the uncertainty bands thus determined are presented both for the B -hadron FFs and for the physical observables evaluated with them.

IV. RESULTS AND DISCUSSION

We are now in a position to present our results for the B -hadron FFs both at NLO and NNLO and to compare the resulting theoretical predictions with the experimental data fitted to, so as to check directly the consistency and goodness of our fits. We also compare our B -hadron FFs with the NLO ones presented by Kniehl, Kramer, Schienbein and Spiesberger (KKSS) [18].

In Table I, for each of the four experimental data sets n , from ALEPH [19], DELPHI [22], OPAL [20], and SLD [21], the number N_n^{data} of data points included in the NLO and NNLO fits and the normalization factors \mathcal{N}_n and the $\chi_n^2(p)$ values thus obtained are specified together with the total number of data points and the values of $\chi_{\text{global}}^2(p)$ and $\chi_{\text{global}}^2(p)/\text{d.o.f.}$ There are $59 - 3 = 56$ degrees of freedom. The NLO and NNLO fits are both excellent, with $\chi_{\text{global}}^2(p)/\text{d.o.f.}$ values of order unity. As expected on general grounds, $\chi_{\text{global}}^2(p)/\text{d.o.f.}$ is reduced as one passes from NLO to NNLO. This is also true for the individual data sets, except for the most recent one, from DELPHI. The NLO and NNLO fit results for p are summarized in Table. II.

In Fig. 1, the z distributions of the NLO and NNLO $b \rightarrow B$ FFs at the initial scale $\mu_F = \mu_0$ are compared with each other. The NLO and NNLO results agree in shape and position of maximum, but differ in normalization. This difference is induced by the $\mathcal{O}(\alpha_s^2)$ correction terms in the hard-scattering cross sections and in the timelike splitting functions, and it is compensated in the physical cross sections to be compared with the experimental data up to terms beyond $\mathcal{O}(\alpha_s^2)$. The error bands determined as described in Sec. III are also shown in Fig. 1. They are dominated by the experimental errors, which explains why they are not reduced by passing from NLO to NNLO. In Fig. 1, the KKSS $b \rightarrow B$ FF [18] is included for comparison. It somewhat undershoots our NLO $b \rightarrow B$ FF, which we attribute to the

impact of the DELPHI data [22], which were not available at the time of the analysis in Ref. [18].

In Fig. 2(a), the analysis of Fig. 1 is repeated for $\mu_F = M_Z$, the CM energy of the experimental data fitted to. Our NLO and NNLO $b \rightarrow B$ FFs are now closer together, the remaining difference being entirely due to the $\mathcal{O}(\alpha_s^2)$ corrections to the hard-scattering cross sections. On the other hand, the difference between the NLO $b \rightarrow B$ FF and the KKSS one is hardly affected by the DGLAP evolution from μ_0 to M_Z , as it is due to a difference in the collection of experimental data fitted to. Figure 2(b) is the counterpart of Fig. 2(a) for the $g \rightarrow B$ FF, which is generated by DGLAP evolution from the initial condition $D_g^B(z, \mu_0) = 0$, as explained in Sec. II. Our NLO and NNLO results are now very similar; the KKSS result again falls below our NLO result. The comparisons between our NLO and NNLO results for the $b \rightarrow B$ and $g \rightarrow B$ FFs are refined in Figs. 2(c) and (d), respectively, where these FFs and their error bands are normalized with respect to the central values at NLO. Deviations occur at small and large values of z , which are outside the focus of our present study. They are due to large soft-gluon and threshold logarithms, respectively, which are included through $\mathcal{O}(\alpha_s^2)$ at NNLO, but only to $\mathcal{O}(\alpha_s)$ at NLO. These logarithms invalidate the fixed-order treatment at small and large values of z and should

TABLE I. Numbers N_n^{data} of data points from data set n included in the NLO and NNLO fits and normalization factors \mathcal{N}_n and χ_n^2 values thus obtained; total number of data points; $\chi_{\text{global}}^2(p)$ values; and $\chi_{\text{global}}^2(p)/\text{d.o.f.}$ values.

Collaboration	N_n^{data}	$\mathcal{N}_n^{\text{NLO}}$	$\mathcal{N}_n^{\text{NNLO}}$	$\chi_n^{2,\text{NLO}}$	$\chi_n^{2,\text{NNLO}}$
ALEPH [19]	18	1.0008	1.0011	14.376	12.269
DELPHI [22]	8	0.9993	1.0058	7.535	15.377
OPAL [20]	15	0.9951	0.9958	35.594	20.002
SLD [21]	18	1.0030	0.9996	25.675	14.195
Total	59			83.180	61.844
$\chi_{\text{global}}^2(p)/\text{d.o.f.}$				1.485	1.104

TABLE II. Values of the fit parameters in Eq. (4) obtained at NLO and NNLO.

Order	N_b	α_b	β_b
NLO	2575.014	15.424	2.394
NNLO	1805.896	14.168	2.341

be resummed. This is, however, beyond the scope of our present analysis and left for future work.

In Fig. 3, the NLO and NNLO results for $(1/\sigma_{\text{tot}})d\sigma(e^+e^- \rightarrow B + X)/dx_B$ evaluated with our respective B -hadron FF sets are compared with the experimental data fitted to. The uncertainty bands stem from those of the B -hadron FFs and are of experimental origin. We observe that the experimental data are in good mutual agreement and are well described both by the NLO and NNLO results down to x_B values of 0.4, say, as for both line shape and normalization. The NNLO description does somewhat better at lower values of x_B , which explains the lower value of $\chi^2_{\text{global}}(p)/\text{d.o.f.}$ in Table I. The failure of the theoretical descriptions in the small- x_B regime is, of course, a direct consequence of the small- x_B cuts applied.

For better visibility, we present the information contained in Fig. 3 as data over theory plots in Fig. 4, one for each experiment. Specifically, the experimental data are in turn normalized to the NLO and NNLO central values. As already explained above, the NLO and NNLO uncertainty bands are very similar. As already visible in Fig. 3, the experimental data consistently undershoot the NLO and NNLO results in the small- x_B regime. On the other hand, their large- x_B behavior is nonuniform. While the ALEPH and OPAL data overshoot the NLO and NNLO results in the upper x_B range, there is nice agreement for the DELPHI and SLD data.

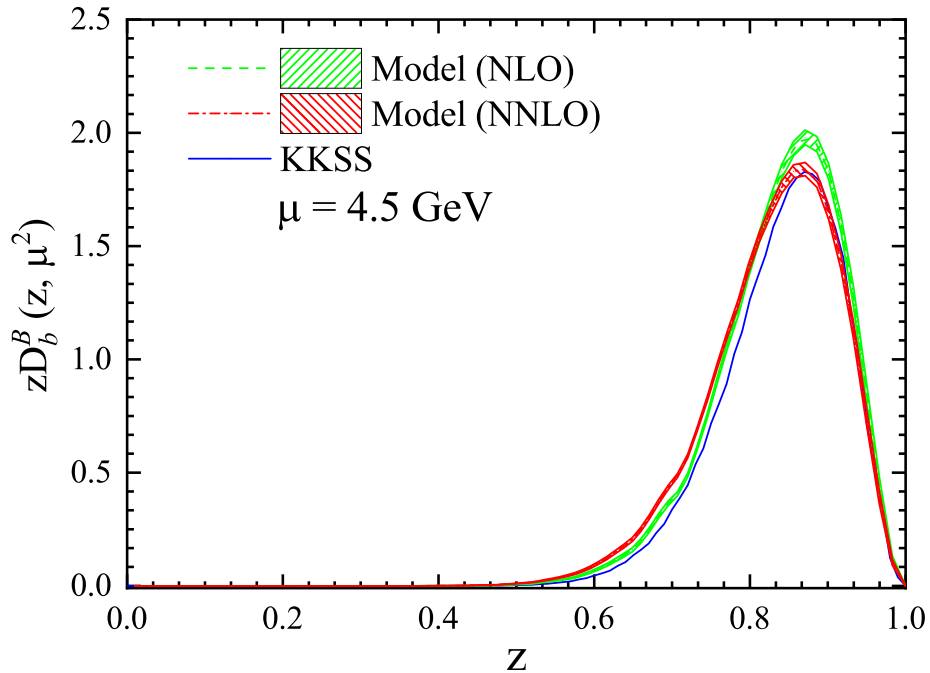


FIG. 1. Line shapes of $zD_b^B(z, \mu_0)$ with $\mu_0 = 4.5$ GeV at NLO (green dashed line) and NNLO (red dot-dashed line) and their experimental uncertainty bands (green and red hatched areas). The KKSS result [18] (blue solid line) is shown for comparison.

V. *B*-HADRON PRODUCTION BY TOP-QUARK DECAY

As a topical application of our *B*-hadron FFs, we study inclusive single *B*-hadron production at the LHC. *B* hadrons may be produced directly or through the decay of heavier particles, including the *Z* boson, the Higgs boson, and the top quark. For definiteness, we concentrate here on the latter process, $t \rightarrow BW^+ + X$, where *X* collectively denotes any other final-state particles. This allows one to study properties of the top quark, such

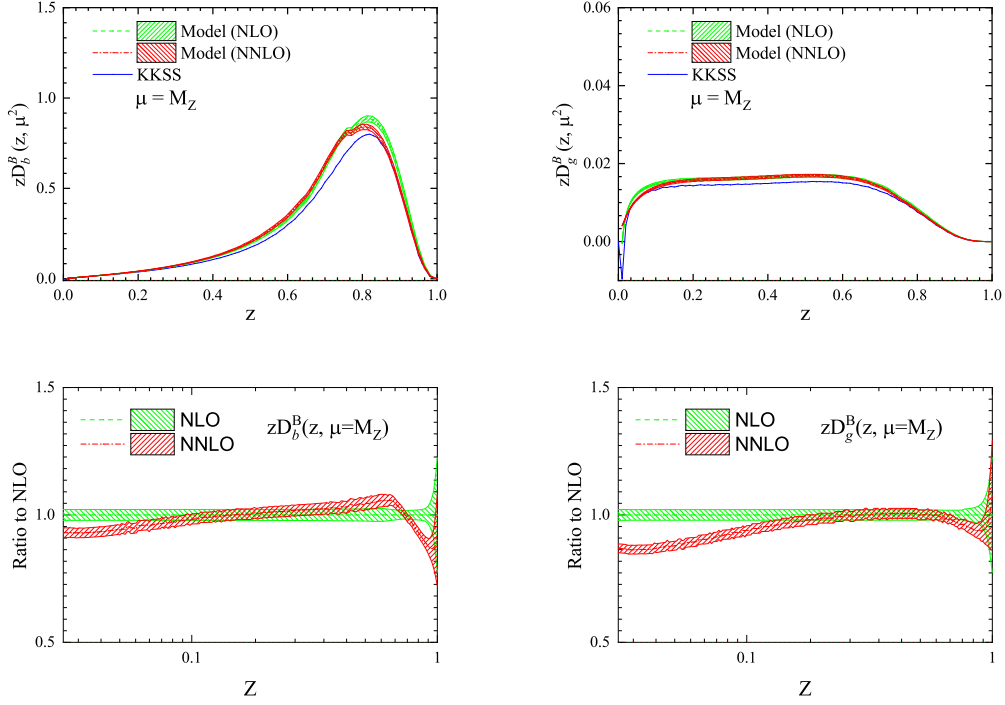


FIG. 2. Line shapes of (a) $zD_b^B(z, M_Z)$ and (b) $zD_g^B(z, M_Z)$ at NLO (green dashed lines) and NNLO (red dot-dashed lines) and their experimental uncertainty bands (green and red hatched areas). The KKSS results [18] (blue solid lines) are shown for comparison. NLO and NNLO results for (c) $zD_b^B(z, M_Z)$ and (d) $zD_g^B(z, M_Z)$ normalized with respect to the NLO central values.

as its degree of polarization in a given production mode, which includes single and pair production. We thus consider both unpolarized and polarized top quarks.

We work in the rest frame of the top quark. The partial width of the decay $t \rightarrow BW^+ + X$, differential in the scaled B -hadron energy x_B and the angle θ_P enclosed between the top-quark polarization three-vector \vec{P} and the B -hadron three-momentum \vec{p}_B is given by

$$\frac{d^2\Gamma}{dx_B d\cos\theta_P}(t \rightarrow BW^+ + X) = \frac{1}{2} \left(\frac{d\Gamma^{\text{unpol}}}{dx_B} + P \frac{d\Gamma^{\text{pol}}}{dx_B} \cos\theta_P \right), \quad (8)$$

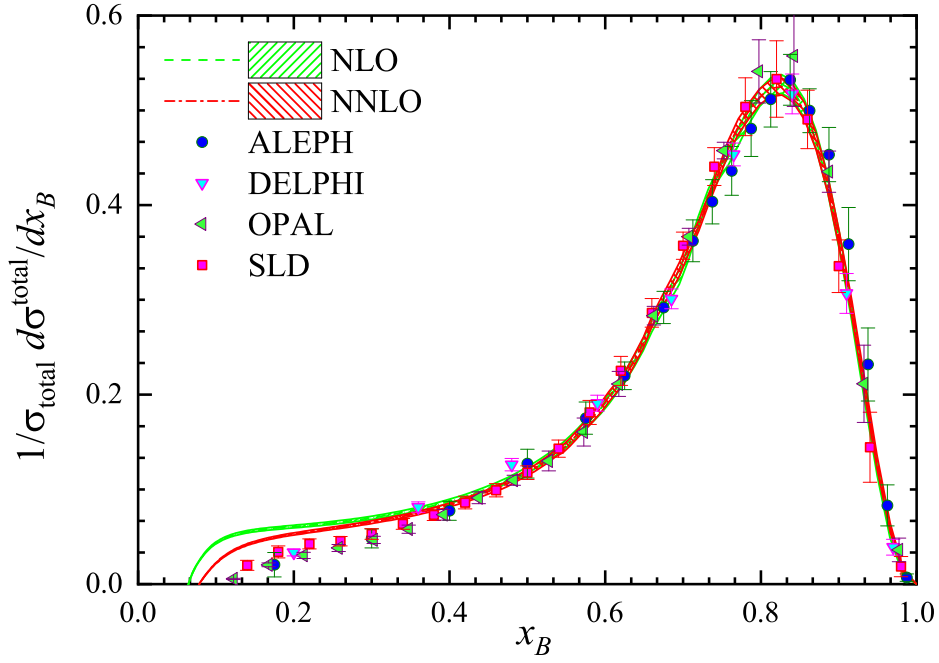


FIG. 3. The NLO (green dashed line) and NNLO (red dot-dashed line) results for $(1/\sigma_{\text{tot}})d\sigma(e^+e^- \rightarrow B + X)/dx_B$ evaluated with our respective B -hadron FF sets are compared with the experimental data fitted to, from ALEPH [19], DELPHI [22], OPAL [20], and SLD [21]. The uncertainty bands (green and red hatched areas) stem from those of the B -hadron FFs.

where $P = |\vec{P}|$ is the degree of polarization. In the ZM-VFNS, we have

$$\frac{d\Gamma^{\text{unpol/pol}}}{dx_B} = \sum_{i=b,g} \int_{x_i^{\min}}^{x_i^{\max}} \frac{dx_i}{x_i} \frac{d\Gamma_i^{\text{unpol/pol}}}{dx_i}(x_i, \mu_R, \mu_F) D_i^B\left(\frac{x_B}{x_i}, \mu_F\right), \quad (9)$$

where $d\Gamma_i^{\text{unpol}}/dx_i$ and $d\Gamma_i^{\text{pol}}/dx_i$ refer to the parton-level decay $t \rightarrow iW^+ + X$, differential in the scaled energy x_i of parton $i = b, g$. In the top-quark rest frame, we have $x_B = E_B/E_b^{\max}$ and $x_i = E_i/E_b^{\max}$, where E_B and E_i are the energies of the B hadron and parton i , and E_b^{\max}

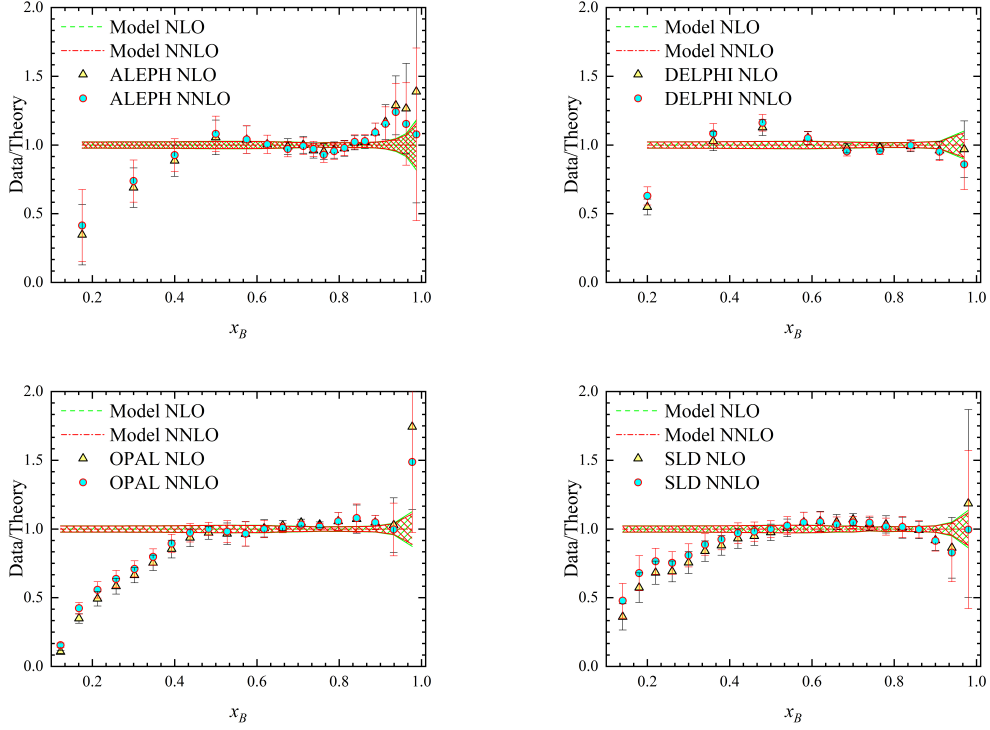


FIG. 4. (a) ALEPH [19], (b) DELPHI [22], (c) OPAL [20], and (d) SLD [21] data of $(1/\sigma_{\text{tot}})d\sigma(e^+e^- \rightarrow B + X)/dx_B$ normalized with respect to our NLO (green hatched bands) and NNLO (red hatched bands) results.

is the maximum energy of the bottom quark. In our application of the ZM-VFNS, where $m_b \ll \mu_F = \mathcal{O}(m_t)$, the bottom quark is taken to be massless. By the same token, we also neglect the B -hadron mass m_B . So far, $d\Gamma_i^{\text{unpol}}/dx_i$ and $d\Gamma_i^{\text{pol}}/dx_i$ are only available through NLO; analytic expressions may be found in Refs. [32–34] and Refs. [35–38], respectively. In Ref. [38], θ_p is taken to be enclosed between \vec{P} and the W -boson three-momentum \vec{p}_W . Although a consistent analysis is presently limited to NLO, we also employ our NNLO B -hadron FF set to explore the possible size of the NNLO corrections.

In our numerical analysis, we use $m_b = 4.5$ GeV, $m_W = 80.379$ GeV, and $m_t = 173.0$ GeV [26], and choose $\mu_R = \mu_F = m_t$. In Fig. 5(a), we present the NLO predictions of $d\Gamma^{\text{unpol}}/dx_B$ and $d\Gamma^{\text{pol}}/dx_B$, evaluated with our NLO B -hadron FF set. For comparison, the evaluations with our NNLO B -hadron FF set are also included. We observe from Fig. 5(a) that switching from the NLO B -hadron FF set to the NNLO one slightly smoothens the theoretical prediction, decreasing it in the peak region and increasing it in the tail region thereunder. At the same time, the peak position is shifted towards smaller values of x_B . The change in normalization is of order 5% at most. These effects should mark an upper limit of the total NNLO corrections because the as-yet-unknown NNLO corrections to $d\Gamma_i^{\text{unpol}}/dx_i$ and $d\Gamma_i^{\text{pol}}/dx_i$ are expected to give rise to some compensation if FF universality is realized in nature. In Fig. 5(b), the results for $d\Gamma^{\text{pol}}/dx_B$ in Fig. 5(a) are compared to the evaluation with the KKSS B -hadron FF set [18]. As in Figs. 1, 2(a), and 2(b), the NLO result is somewhat reduced by switching to the KKSS B -hadron FF set.

VI. SUMMARY AND CONCLUSIONS

In this paper, we determined nonperturbative FFs for B hadrons, both at NLO and NNLO in the ZM-FVNS, by fitting to all available experimental data of inclusive single B -hadron production in e^+e^- annihilation, $e^+e^- \rightarrow B + X$, from ALEPH [19], DELPHI [22], OPAL [20], and SLD [21]. We then applied these B -hadron FFs to provide NLO predictions for inclusive B -hadron production by top-quark decay, $t \rightarrow BW^+ + X$, both for unpolarized and polarized top quarks.

Our analysis updates and improves similar ones in the literature [17, 18] in the following respects. We included the DELPHI data [22], which had not been available then. For the first time, we advanced to NNLO in a fit of B -hadron FFs. We performed a careful estimation of the experimental uncertainties in our B -hadron FFs using the Hessian approach.

We adopted the simple power ansatz of Eq. (4) and obtained for the three fit parameters

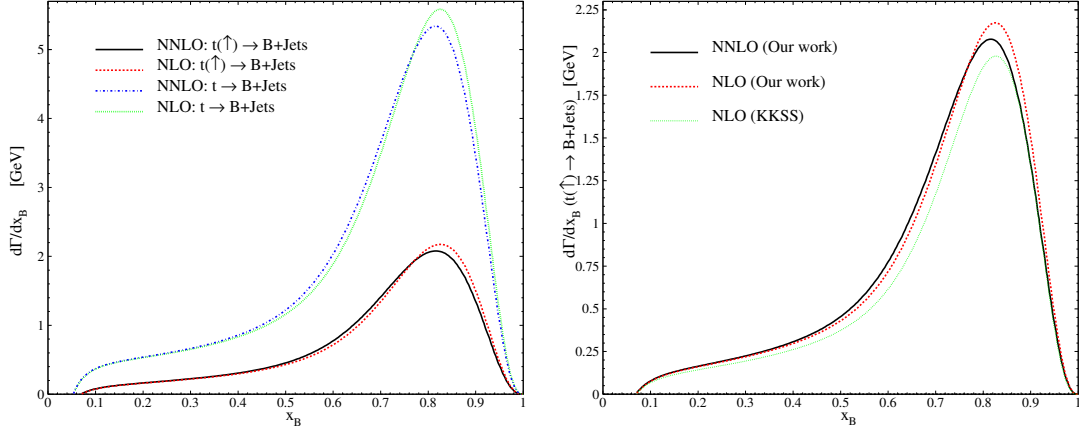


FIG. 5. (a) NLO predictions of $d\Gamma^{\text{unpol}}/dx_B$ (green dotted line) and $d\Gamma^{\text{pol}}/dx_B$ (red dashed line), evaluated with our NLO B -hadron FF set. For comparison, the evaluations with our NNLO B -hadron FF set are also included (blue dot-dashed and black solid lines). (b) The results for $d\Gamma^{\text{pol}}/dx_B$ in Fig. 5(a) are compared to the evaluation with the KKSS B -hadron FF set [18] (green dotted line).

appearing therein the values listed in Table II. The goodness of the NLO and NNLO fits turned out to be excellent, with $\chi^2/\text{d.o.f.}$ values of 1.485 and 1.104, respectively (see Table I). As expected on general grounds, the fit quality is improved by ascending to higher orders of perturbation theory.

We encourage the LHC Collaborations to measure the x_B distribution of the partial width of the decay $t \rightarrow BW^+ + X$, for two reasons. On the one hand, this will allow for an independent determination of the B -hadron FFs and thus provide a unique chance to test their universality and DGLAP scaling violations, two important pillars of the QCD-improved parton model of QCD. On the other hand, this will allow for a determination of the top-quark polarization, which should depend on the production mode.

The theoretical framework provided by the ZM-FVNS was quite appropriate for the present analysis, since the characteristic energy scales of the considered processes, M_Z and

m_t , greatly exceeded the bottom-quark mass m_b , which could thus be neglected. Possible theoretical improvements include the inclusion of finite- m_b and finite- m_B effects, and the resummation of soft-gluon logarithms, which extend the validity towards small values of x_B , and the resummation of threshold logarithms, which extends the validity towards large values of x_B . The general-mass variable-flavor-number scheme (GM-VFNS) [39–42] provides a consistent and natural finite- m_b generalization of the ZM-VFNS on the basis of the $\overline{\text{MS}}$ factorization scheme [43]. The processes considered here, $e^+e^- \rightarrow B + X$ [44], $t \rightarrow BW^+ + X$ [34], and $t(\uparrow) \rightarrow BW^+ + X$ [45], have all been worked out in the GM-VFNS at NLO, but not yet at NNLO. Finite- m_B effects may be conveniently incorporated using the approach of Refs. [46–48]. The implementation of such theoretical improvements reaches beyond the scope of the present analysis and is left for future work.

ACKNOWLEDGMENTS

Hamzeh Khanpour and Maryam Soleymaninia thank the School of Particles and Accelerators at the Institute for Research in Fundamental Sciences (IPM) for financial support. Hamzeh Khanpour is also grateful to the University of Science and Technology of Mazandaran for financial support. This work was supported in part by the German Federal Ministry for Education and Research (BMBF) through Grant No. 05H18GUCC1.

-
- [1] C. Albajar *et al.* [UA1 Collaboration], Phys. Lett. B **213**, 405 (1988). doi:10.1016/0370-2693(88)91785-6
 - [2] V. N. Gribov and L. N. Lipatov, Sov. J. Nucl. Phys. **15**, 438 (1972) [Yad. Fiz. **15**, 781 (1972)].
 - [3] G. Altarelli and G. Parisi, Nucl. Phys. B **126**, 298 (1977). doi:10.1016/0550-3213(77)90384-4
 - [4] Y. L. Dokshitzer, Sov. Phys. JETP **46**, 641 (1977) [Zh. Eksp. Teor. Fiz. **73**, 1216 (1977)].
 - [5] A. Mitov, S. Moch and A. Vogt, Phys. Lett. B **638**, 61 (2006) doi:10.1016/j.physletb.2006.05.005 [hep-ph/0604053].

- [6] S. Moch and A. Vogt, Phys. Lett. B **659**, 290 (2008) doi:10.1016/j.physletb.2007.10.069 [arXiv:0709.3899 [hep-ph]].
- [7] A. A. Almasy, S. Moch and A. Vogt, Nucl. Phys. B **854**, 133 (2012) doi:10.1016/j.nuclphysb.2011.08.028 [arXiv:1107.2263 [hep-ph]].
- [8] P.J. Rijken and W. L. van Neerven, Phys. Lett. B **386**, 422 (1996) doi:10.1016/0370-2693(96)00898-2 [hep-ph/9604436].
- [9] P. J. Rijken and W. L. van Neerven, Phys. Lett. B **392**, 207 (1997) doi:10.1016/S0370-2693(96)01529-8 [hep-ph/9609379].
- [10] P. J. Rijken and W. L. van Neerven, Nucl. Phys. B **487**, 233 (1997) doi:10.1016/S0550-3213(96)00669-4 [hep-ph/9609377].
- [11] A. Mitov and S. O. Moch, Nucl. Phys. B **751**, 18 (2006) doi:10.1016/j.nuclphysb.2006.05.018 [hep-ph/0604160].
- [12] D. P. Anderle, F. Ringer and M. Stratmann, Phys. Rev. D **92**, no. 11, 114017 (2015) doi:10.1103/PhysRevD.92.114017 [arXiv:1510.05845 [hep-ph]].
- [13] V. Bertone *et al.* [NNPDF Collaboration], Eur. Phys. J. C **77**, no. 8, 516 (2017) doi:10.1140/epjc/s10052-017-5088-y [arXiv:1706.07049 [hep-ph]].
- [14] M. Soleymaninia, M. Goharipour and H. Khanpour, Phys. Rev. D **98**, no. 7, 074002 (2018) doi:10.1103/PhysRevD.98.074002 [arXiv:1805.04847 [hep-ph]].
- [15] M. Soleymaninia, M. Goharipour and H. Khanpour, Phys. Rev. D **99**, no. 3, 034024 (2019) doi:10.1103/PhysRevD.99.034024 [arXiv:1901.01120 [hep-ph]].
- [16] M. Soleymaninia, H. Khanpour and S. M. Moosavi Nejad, Phys. Rev. D **97**, no. 7, 074014 (2018) doi:10.1103/PhysRevD.97.074014 [arXiv:1711.11344 [hep-ph]].
- [17] J. Binnewies, B. A. Kniehl and G. Kramer, Phys. Rev. D **58**, 034016 (1998) doi:10.1103/PhysRevD.58.034016 [hep-ph/9802231].
- [18] B. A. Kniehl, G. Kramer, I. Schienbein and H. Spiesberger, Phys. Rev. D **77**, 014011 (2008) doi:10.1103/PhysRevD.77.014011 [arXiv:0705.4392 [hep-ph]].
- [19] A. Heister *et al.* [ALEPH Collaboration], Phys. Lett. B **512**, 30 (2001) doi:10.1016/S0370-2693(01)00690-6 [hep-ex/0106051].
- [20] G. Abbiendi *et al.* [OPAL Collaboration], Eur. Phys. J. C **29**, 463 (2003) doi:10.1140/epjc/s2003-01229-x [hep-ex/0210031].
- [21] K. Abe *et al.* [SLD Collaboration], Phys. Rev. D **65**, 092006 (2002) Erratum: [Phys. Rev.

- D **66**, 079905 (2002)] doi:10.1103/PhysRevD.66.079905, 10.1103/PhysRevD.65.092006 [hep-ex/0202031].
- [22] J. Abdallah *et al.* [DELPHI Collaboration], Eur. Phys. J. C **71**, 1557 (2011) doi:10.1140/epjc/s10052-011-1557-x [arXiv:1102.4748 [hep-ex]].
- [23] J. Pumplin, D. R. Stump and W. K. Tung, Phys. Rev. D **65**, 014011 (2001) doi:10.1103/PhysRevD.65.014011 [hep-ph/0008191].
- [24] K. G. Chetyrkin, A. L. Kataev and F. V. Tkachov, Phys. Lett. **85B**, 277 (1979). doi:10.1016/0370-2693(79)90596-3
- [25] V. G. Kartvelishvili and A. K. Likhoded, Yad. Fiz. **42**, 1306 (1985) [Sov. J. Nucl. Phys. **42**, 823 (1985)].
- [26] M. Tanabashi *et al.* [Particle Data Group], Phys. Rev. D **98**, no. 3, 030001 (2018). doi:10.1103/PhysRevD.98.030001
- [27] D. Stump, J. Pumplin, R. Brock, D. Casey, J. Huston, J. Kalk, H. L. Lai and W. K. Tung, Phys. Rev. D **65**, 014012 (2001) doi:10.1103/PhysRevD.65.014012 [hep-ph/0101051].
- [28] J. Blumlein, H. Bottcher and A. Guffanti, Nucl. Phys. B **774**, 182 (2007) doi:10.1016/j.nuclphysb.2007.03.035 [hep-ph/0607200].
- [29] F. James and M. Roos, Comput. Phys. Commun. **10**, 343 (1975). doi:10.1016/0010-4655(75)90039-9
- [30] V. Bertone, S. Carrazza and J. Rojo, Comput. Phys. Commun. **185**, 1647 (2014) doi:10.1016/j.cpc.2014.03.007 [arXiv:1310.1394 [hep-ph]].
- [31] A. D. Martin, W. J. Stirling, R. S. Thorne and G. Watt, Eur. Phys. J. C **63**, 189 (2009) doi:10.1140/epjc/s10052-009-1072-5 [arXiv:0901.0002 [hep-ph]].
- [32] G. Corcella and A. D. Mitov, Nucl. Phys. B **623**, 247 (2002) doi:10.1016/S0550-3213(01)00639-3 [hep-ph/0110319].
- [33] M. Cacciari, G. Corcella and A. D. Mitov, JHEP **0212**, 015 (2002) doi:10.1088/1126-6708/2002/12/015 [hep-ph/0209204].
- [34] B. A. Kniehl, G. Kramer and S. M. Moosavi Nejad, Nucl. Phys. B **862**, 720 (2012) doi:10.1016/j.nuclphysb.2012.05.008 [arXiv:1205.2528 [hep-ph]].
- [35] M. Fischer, S. Groote, J. G. Korner, M. C. Mauser and B. Lampe, Phys. Lett. B **451**, 406 (1999) doi:10.1016/S0370-2693(99)00194-X [hep-ph/9811482].
- [36] M. Fischer, S. Groote, J. G. Korner and M. C. Mauser, Phys. Rev. D **65**, 054036 (2002)

- doi:10.1103/PhysRevD.65.054036 [hep-ph/0101322].
- [37] S. M. Moosavi Nejad, Phys. Rev. D **88**, no. 9, 094011 (2013) doi:10.1103/PhysRevD.88.094011 [arXiv:1310.5686 [hep-ph]].
- [38] S. M. Moosavi Nejad and M. Balali, Phys. Rev. D **90** (2014) no.11, 114017 Erratum: [Phys. Rev. D **93** (2016) no.11, 119904] doi:10.1103/PhysRevD.90.114017, 10.1103/PhysRevD.93.119904 [arXiv:1409.1389 [hep-ph]].
- [39] G. Kramer and H. Spiesberger, Eur. Phys. J. C **22**, 289 (2001) doi:10.1007/s100520100805 [hep-ph/0109167].
- [40] B. A. Kniehl, G. Kramer, I. Schienbein and H. Spiesberger, Phys. Rev. D **71**, 014018 (2005) doi:10.1103/PhysRevD.71.014018 [hep-ph/0410289].
- [41] B. A. Kniehl, G. Kramer, I. Schienbein and H. Spiesberger, Eur. Phys. J. C **41**, 199 (2005) doi:10.1140/epjc/s2005-02200-7 [hep-ph/0502194].
- [42] B. A. Kniehl, G. Kramer, I. Schienbein and H. Spiesberger, Phys. Rev. Lett. **96**, 012001 (2006) doi:10.1103/PhysRevLett.96.012001 [hep-ph/0508129].
- [43] J. C. Collins, Phys. Rev. D **58**, 094002 (1998) doi:10.1103/PhysRevD.58.094002 [hep-ph/9806259].
- [44] T. Kneesch, B. A. Kniehl, G. Kramer and I. Schienbein, Nucl. Phys. B **799**, 34 (2008) doi:10.1016/j.nuclphysb.2008.02.015 [arXiv:0712.0481 [hep-ph]].
- [45] S. M. Moosavi Nejad and M. Balali, Eur. Phys. J. C **76**, no. 3, 173 (2016) doi:10.1140/epjc/s10052-016-4017-9 [arXiv:1602.05322 [hep-ph]].
- [46] S. Albino, B. A. Kniehl, G. Kramer and W. Ochs, Phys. Rev. D **73**, 054020 (2006) doi:10.1103/PhysRevD.73.054020 [hep-ph/0510319].
- [47] S. Albino, B. A. Kniehl, G. Kramer and C. Sandoval, Phys. Rev. D **75**, 034018 (2007) doi:10.1103/PhysRevD.75.034018 [hep-ph/0611029].
- [48] S. Albino, B. A. Kniehl and G. Kramer, Nucl. Phys. B **803**, 42 (2008) doi:10.1016/j.nuclphysb.2008.05.017 [arXiv:0803.2768 [hep-ph]].